15TH IEA HEAT PUMP CONFERENCE
MAY 26–29, 2026 | HOFBURG
VIENNA 2026
DECARBONISATION THROUGH INNOVATION

Optimized integration concepts for basic-booster heat pump solutions for building renovations

Gerald Zotter[a], Franz Hengel [a], Johanna Roth [a], Manuel Früh [a], Catlina Elsa Olivas[b]

[a]AEE INTEC, A-8200 Gleisdorf, Feldgasse 19, Austria
[b]TECNOLÓGICO DE MONTERREY, AV. EUGENIO GARZA SADA 2501 COL. TECNOLÓGICO C.P. 64700 | MONTERREY, NUEVO LEÓN, MÉXICO

Abstract

Achieving climate-neutral cities in Europe requires replacing of gas-fired boilers with efficient heating systems that can be integrated into existing older apartment buildings. In addition to district heating, basic-booster heat pumps combined with minimally invasive thermal refurbishment of old buildings are essential. Because the performance of heat pumps depends largely on the required temperature lift, they are typically paired with floor heating systems. In building renovation, however, such solutions as changing from radiators to floor heating systems is often overly invasive. Therefore, it is essential to retain existing radiators while reducing supply temperatures below 45 °C through targeted thermal refurbishment. This work presents detailed simulations to assess the performance of basic-booster heat pump systems and optimize the design of intermediate heating circuits. The results show that basic-booster heat pumps can achieve up to 25% higher coefficients of performance compared to single-stage systems. Optimal performance is obtained by appropriately sizing the central basic heat pump, minimizing the temperature spread, and matching the temperature level of the intermediate circuit to the intermediate pressure level of a comparable two-stage cycle. An intermediate storage tank enables the system to use a day-night-shift, which can increase the coefficient of performance by approximately further 10% through the utilization of higher daytime ambient temperatures and reduce nighttime fan noise from air-source units. When properly designed, the basic-booster heat pump system offers an efficient and practical technology to replace gas boilers in building renovations for urban areas.[1]

© HPC2026.
Selection and/or peer-review under the responsibility of the organizers of the 15th IEA Heat Pump Conference 2026.

Keywords: Two-stage cylce, single-satge cycle, cascade, educational innovation,inrermediate circuit, hydraulic integration, propane, EES, 0D-simulation, temperature spread, high temperature lift;

1. Introduction

The phase-out of natural gas is essential for achieving Europe's climate targets and reducing import dependencies, yet space heating in urban multi-family buildings remains strongly locked into gas-based systems. Due to decades of infrastructure development, low investment costs and established practices, gas-fired boilers still dominate the heating stock in many European cities, despite their high lifecycle emissions [1,2].

In dense urban contexts, decarbonisation requires not only CO_2-free heat sources but also building renovation. While building-envelope improvements and heat pumps are widely seen as key solutions, their application in existing apartment buildings is constrained by high supply-temperature requirements, legacy radiator systems, limited accessibility, and highly heterogeneous renovation states [3]. Deep renovations

[1] A shorter German version of parts of this work was presented at a small local conference. I asked the organizer, and they confirmed that I can reuse the content here. Quotes from it were made in the paper.

progress slowly (≈1%/year) and are often economically and socially difficult in occupied multi-family buildings, as they may require relocation and long vacancies [4].

The widespread use of gas-fired floor-standing boilers in individual apartments further complicates the transition, as centralized low-temperature systems typically require invasive changes to distribution systems and emitters. Such interventions approach full gut renovation and are therefore incompatible with the need for rapid, cost-efficient and socially acceptable urban decarbonisation, highlighting the need for minimally invasive and scalable solutions [4].

2. Heat Pump Renovation Strategies for Gas-Heated Multi-Residential Buildings

The following sections discuss state-of-the-art approaches for improving heat-pump efficiency in renovation contexts and introduce the key performance indicators (KPIs) used to assess their performance.

2.1. Heat Pump Renovation Strategies for Gas-Heated Multi-Residential Buildings – Literature review

A comprehensive review of urban retrofits shows that both retrofit depth and emitter characteristics strongly influence the viability of heat pumps (HPs) in older multi-residential buildings, and that combined renovation–system approaches outperform standalone system replacements [6]. Although suitable renovation concepts have existed for years, renovation rates remain at around 1%, mainly due to the need to avoid tenant relocation and long vacancies during deep retrofits [4]. This underlines the need for minimally invasive and scalable renovation methods that can be implemented with minimal disruption.

In multi-storey buildings, the widespread use of decentralised gas-fired apartment boilers further complicates the transition, as most HP alternatives are centralised and would require extensive structural interventions, effectively amounting to major renovations [4]. For this reason, this work focuses on solutions that retain existing radiator systems and avoid invasive distribution-system changes. Among HP options, air-source systems are particularly suitable for urban retrofits due to their lower installation complexity and investment costs [4].

Recent research on high-temperature HPs, cascade concepts, and radiator-compatible emitters shows that the required supply temperatures can be achieved with substantially reduced invasiveness. In particular, cascade HP systems outperform single-stage units in high-temperature retrofit applications due to lower compression ratios and improved operational stability, and are especially suitable for buildings with limited potential to reduce supply temperatures or upgrade insulation [5,7]. Environmental and economic assessments further confirm that HPs achieve substantially lower life-cycle impacts than gas boilers, especially when combined with even moderate envelope improvements [7].

Overall, the literature indicates that cascaded air-source HP systems represent a technically, economically, and ecologically viable pathway for replacing natural-gas boilers in existing multi-residential buildings, provided that system efficiency, investment costs, and energy prices are carefully considered.

2.2. Energetical key performance indicators for heat pumps

The seasonal performance factor (SPF) is used as the measure of efficient operation. The so-called coefficient of performance (COP, see Eq. 1) represents the ratio of the heating capacity ($\dot{Q}_H$) to the electrical input power P_{el}, and provides an indication of the expected SPF—except for the influence of climatic conditions, control strategies, part-load efficiencies, and similar factors—although it is valid only at a steady-state operating point. This COP (see Eq. 2) can be approximated in a simplified form according to Lorenz [8] using the mean entropy-based (logarithmic) source temperature $\bar{T}_{0M}$ (see Eq. 3) and the mean logarithmic sink temperature $\bar{T}_{HM}$ (see Eq. 4). Both temperatures depend on the respective inlet and outlet temperatures ($t_{0,in}$ & $t_{0,out}$) or (t_R & t_S). Together with the Lorenz efficiency factor ν_{Lor}, the COP can thus be estimated based on Eqs. 1 and 2 (Lorenz 1894). The Lorenz efficiency factor ν_{Lor} is defined as the ratio between the actual COP and the simplified Lorenz COP (see Eq. 5). According to [9] and [10], the Lorenz efficiency is preferable to the Carnot efficiency for determining the optimal COP of air-to-water heat pumps, since both the heat source and sink are sensible and no latent heat is involved.

Lower system temperatures are essential for enabling the ecologically and economically viable operation of air-source HPs in existing buildings, including during cold winter periods.

$$COP = \frac{\dot{Q}_H}{P_{el}} \qquad (1)$$

$$COP_{Lor} = \frac{\bar{T}_{HM}}{\bar{T}_{HM} - \bar{T}_{0M}} \qquad (2)$$

$$\bar{T}_{0M} = \frac{t_{0,\mathrm{in}} - t_{0,\mathrm{out}}}{ln\left(\frac{T_{0,\mathrm{in}}}{T_{0,\mathrm{out}}}\right)} \qquad (3)$$

$$\bar{T}_{HM} = \frac{t_{\mathrm{S}} - t_{\mathrm{R}}}{ln\left(\frac{T_{\mathrm{S}}}{T_{\mathrm{R}}}\right)} \qquad (4)$$

$$v_{Lor} = \frac{COP}{COP_{Lor}} \qquad (5)$$

2.3. Heat Pumps for radiator heated old Multi-Residential Buildings without thermal renovation (high U-values)

This section introduces the single-stage air-source heat pump system used in this work as a reference case. It does not represent the target solution for high-temperature radiator systems, but serves as a baseline for quantifying the performance benefits of the cascaded system concept analysed in section 3.

An air-source heat pump (based on the Perkins/Evans cycle with a high-pressure receiver) supplying a radiator-heating application is shown in **Fehler! Verweisquelle konnte nicht gefunden werden.**. **Fehler! Verweisquelle konnte nicht gefunden werden.** shows the HP cycle (in green) in the temperature–enthalpy (t–h) diagram [10]. It involves the compression (black segment on the enthalpy axis) from point 1 to 2, the isobaric condensation (blue/red segment on the enthalpy axis) from 2 to 3, the isenthalpic expansion from 3 to 4, and the isobaric evaporation (green segment on the enthalpy axis) from 4 to 1 [10]. Pressure losses and heat gains/losses have been neglected.[2]

Figure 2 also compares this cycle with the cycle of the floor-heating application (with supply/return temperatures of 32/27°C, dotted line) to those of the radiator application (75/55 °C). As can be seen from the t–h diagram, the heating capacity decreases by approximately 15%, and the required compressor power increases due to the increase of the high-pressure side at constant low-pressure. This leads to the fact that the COP decreases by about 40%. The reason for this is the large temperature lift, which would reduce a COP of about 4 (typical for floor heating) to approximately 2.4 when supplying radiators at 75/55 °C.

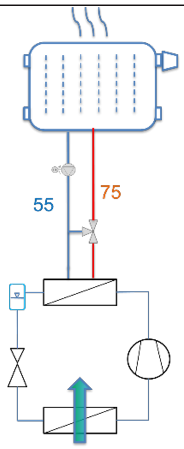

Figure 1: Schematic of a heat pump for radiator heating

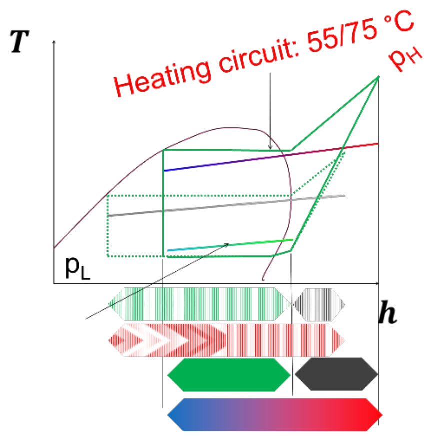

Figure 2: HP cycle in the temperature–enthalpy (T–h) diagram, including the temperature levels of the heat sink for radiator heating (solid lines) in comparison with floor heating (dotted lines, cf. Fig 2, at identical low-pressure conditions). The diagram indicates the specific heating capacity (blue/red), the specific source capacity (green), and the specific compressor work (black). [10]

[2] The t–h diagram is well suited to illustrate the process together with the heat-exchanger diagrams. This makes it possible to visualize the influence of inlet temperatures and mass flow rates of source and sink on the cycle as well as on heat-exchanger sizing. Furthermore, the COP can be read directly as the ratio of the condensation length (blue/red) to the compression length (black), because the same refrigerant mass flow rate ($\dot{m}_{ref}$) passes through all components of the HP.

A detailed simulation study using EES [11], see an example for the cycle analysis in Figure 3, for the refrigerant propane (R290), showed that the COP and the heating capacity are at least 40 % lower at supply/return temperatures of 75/55 °C compared to floor heating assuming the same HP-plant (i.e. same compressor displacement and rotational speed, heat exchanger sizes, throttle and receiver size). The results are summarized in Table 1. For the simulation, an isentropic and volumetric compressor efficiency of 80%, the swept volume was set to 42 ccm and a pinch-point temperature difference of 5 K, as well as superheating temperature of 5 K are an oil ratio of 10% and a mechanical-electrical efficiency of 95% assumed; rotational speed is set point of the simulation but could be adapted to required heat capacity (with maximum of 7200 rpm), as well as required mass flow of air and heating water circuit. The boundaries set in the simulation are a fixed return and supply temperatures and air source inlet temperature as well. A full compressor efficiency map over the entire operating envelope was not considered, and part-load behavior was likewise excluded; consequently, the comparison is limited to the system's design point. If renovation measures were used to reduce the radiator supply temperature to 45 °C, the COP could be increased by approximately 50 % compared to the high supply temperature of 75 °C.

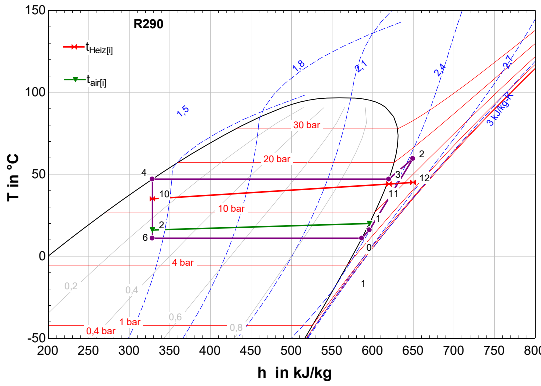

Figure 3: Depiction of the vapor-compression heat pump cycle (purple) in the temperature–enthalpy (T–h) diagram, including the imposed temperature levels of the heat sink (red) and heat source (green), as obtained from the EES (2022) model. [10]

Table 1. Comparison of the COP of single-stage heat pumps using R290 as a function of outdoor air temperature and heating system temperature (excluding defrosting)[3] [10]

Ambient temperature (t_a) in °C	COP @ t_S/t_R 35/29 °C	COP @ t_S/t_R 45/35 °C	COP @ t_S/t_R 75/55 °C
-15	3,1	2,7	1,8
0	4,2	3,5	2,2
7	4,9	4,1	2,5

2.4. Heat Pump for radiator heated old Multi-Residential Buildings with thermal renovation (low U-values)

To counteract the poor COP at high supply temperatures, buildings must undergo thermal renovation in order to reduce the required heating capacity ($\dot{Q}_H$), below the one without thermal renovation ($\dot{Q}_{H\_100}$). This reduction in heating demand ($\dot{Q}_H/\dot{Q}_{H\_100}$) also lowers the required radiator output, thereby reducing the necessary supply and return temperatures for a given heat-emitter surface area. Eq. (6) shows the heating load as a function of transmission losses ($\dot{Q}_T$) and ventilation losses ($\dot{Q}_L$). Both losses depending mainly on the inner room temperature (t_i) and the ambient temperature (t_a), see Eq. 6 and Eq. 7. $\dot{Q}_T$ also depends on the surface of the building and its U-Values (from walls over windows to the roof). $\dot{Q}_L$ depends also on the volume (V) of the buildings and air change rate (ACH), as well as of the density (ρ) and heat capacity ($c_{p,l}$) of the air. Eq. 9 illustrates the change in radiator output as a function of the logarithmic temperature difference (Eq. 10, which is determined by t_S/t_R and t_i) and the heat-emission exponent (n).

$$\dot{Q}_T = \sum UA(t_i - t_a) \tag{6}$$
$$\dot{Q}_L = ACH * V * \rho * c_{p,l}(t_i - t_a) \tag{7}$$
$$\dot{Q}_H = \dot{Q}_T + \dot{Q}_L \tag{8}$$
$$\frac{\dot{Q}_H}{\dot{Q}_{H\_100}} = \left(\frac{\Delta T_{ln}}{\Delta T_{ln\_100}}\right)^n \tag{9}$$

[3] Only the design point operation was considered for the comparison. Defrosting effects were not considered on the air-source heat pump (for the design point of -15 °C irrelevant, but relevant for ambient temperature around 3 °C).

$$\Delta T_{ln} = \frac{t_S - t_R}{ln\left(\frac{t_S - t_i}{t_R - t_i}\right)} \quad (10)$$

Considering that the radiator output must match the required heating load, and assuming that the heating-water volumetric flow rate remains unchanged due to the existing piping, Figure 6 indicates that the heating load must be reduced by approximately 60 % through thermal renovation in order to lower the required supply temperature below 45 °C [10]. As shown in Table 1, this would enable acceptable COP values. However, single-stage heat pumps based on the Perkins/Evans cycle generally struggle to handle high temperature lifts, owing to limitations imposed by the refrigerant's pressure levels and critical point, as well as restrictions arising from the compressor operating envelope, which ultimately results in low COPs.

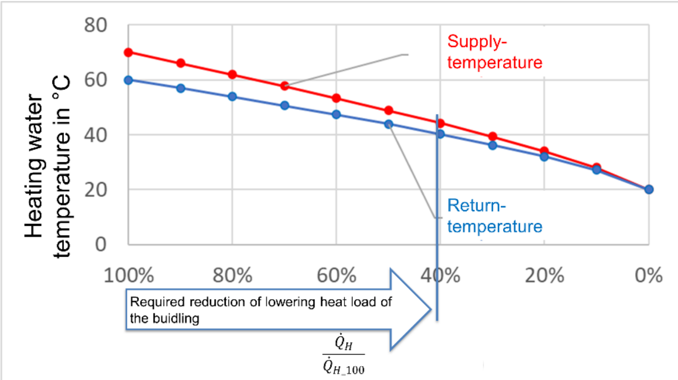

Figure 4: The graph shows how the required heating-water temperatures (supply and return) decrease as the building's heating load is reduced through thermal renovation. The required supply and return temperatures of the heating system depend on the ratio of the actual heating load to the heating load of the building that has not been renovated. 100% of the ratio corresponds to the original heating load of the non-renovated building. The analysis is based on an existing radiator system with a heat exchanger exponent of n=1.3 [10]

3. Basic-booster heat pumps concepts for renovation strategies of old multi-residential buildings

An additional alternative is the basic-booster HP solutions [12] & [13]. These solutions can be considered for domestic hot water production due to the high temperatures of around 60 °C required [14]. However, when the required heating temperature level is higher than that of underfloor heating, booster heat pumps can be used together with a central basic heat pump for heating and/or domestic hot water supply in multi-storey residential buildings.

3.1. Comparison of basic-booster with a single-stage heat pump

Compared to the single-stage central heat pump (Figure 7), the booster HPs access the heat source via a basic HP through a low-temperature heating rail (yellow/turquoise in Figure 8, also called intermediate circuit in this paper). This means the concept is a cascade system, in which the low-temperature condenser is coupled with the high-pressure evaporator via the intermediate circuit (low-temperature heating circuit of the basic HP).

To evaluate the overall COP of the entire basic-booster HP system, the so-called $\mathrm{COP_{total}}$ is used, considering the ration of heat capacity ($\dot{Q}_H$) compared to the electrical power consumption of both HPs, the basic HP (P_{el_Basic}) and the booster HP ($P_{el\_Booster}$), see Eq. 11. Using this basic-booster system to achieve higher COPs compared to the single-stage central HP so that $\mathrm{COP_{total}}$ becomes higher than the COP of the single-stage central system, according to the first law of thermodynamics, the source heat input in the basic HP must be higher than in single-stage central systems (see Eq. 12 & 13). Assuming that the compressor power input of both systems is the same, $\mathrm{COP_{total}}$ can be expressed in terms of the individual partial COPs of the booster and basic heat pumps, as formulated in Eq. 14. Consequently, the partial COPs of the cascade must be almost twice as high as the required $\mathrm{COP_{total}}$. This can be achieved but only if the system is well designed, as explained in this chapter. The design point of the intermediate circuit has to be well determined in order that the temperature lifts are as low so that $COP_{Basic} > 2 * COP_{single-stage}$ and $COP_{Booster} > 2 * COP_{single-stage}$.

$$COP_{total} = \frac{\dot{Q}_H}{P_{el\_Booster} + P_{el\_Basic}} \quad (11)$$

$$\dot{Q}_0 = \dot{Q}_H * \frac{COP}{COP-1} \tag{12}$$

$$If\ \dot{Q}_{0\_Basic} > \dot{Q}_{0single-stage} \rightarrow COP_{total} > COP_{single-stage} \tag{13}$$

$$COP_{total} = \frac{COP_{Booster}}{2} \_ \frac{COP_{Basic}-1}{2} \tag{14}$$

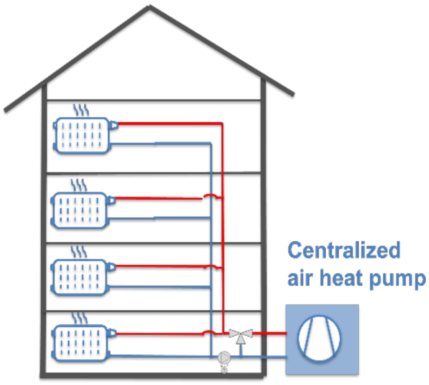

Figure 5: Schematic of one centralized heat pump concept for multi-storey residential buildings with radiators [10]

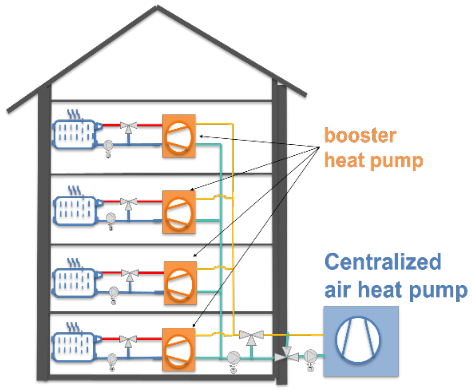

Figure 6: Schematic of one centralized heat pump as basic heat pump and booster heat pumps in each flat as HP concept for multi-storey residential buildings with radiators [10]

3.2. Comparison of basic/booster HPs with a two-stage heat pump

Although the basic–booster HPs operate in a cascaded configuration, both heat pumps usually use the same refrigerant (see Fig. 9 and Fig. 10[4]), such as propane. Consequently, the ideal thermodynamic cycle corresponds to a two-stage vapor-compression cycle, which represents the maximum achievable COP ($COP_{two\text{-}stage}$) for this configuration, as no additional intermediate circuit (low-temperature circuit) is required. Therefore, no twofold pinch-point temperature difference is necessary between the condenser of the basic HP and the intermediate circuit and the evaporator of the booster HP (see Fig. 11 and Fig. 12) [10].

From this maximum, the ideal temperature level of the intermediate circuit can be derived. Based on the ideal intermediate pressure level (p_M), defined by equal pressure ratios across both compressors (Eq. 15), this temperature level corresponds to the saturation temperature associated with p_M for the chosen refrigerant (Eq. 16). For propane, this saturation temperature is approximately 20 °C, although it varies with the outdoor air temperature [10]. The low temperature level of it also contributes to reduced thermal losses in a possible storage tank (typically located in the basement). Furthermore, the temperature spread in the low-temperature loop should ideally approach zero to maximize the overall COP (COP_{total}), which would mean that an infinite high pump mass flow would be requested. So, a temperature spread of max. 3K is suggested for high performance and suitable pump mass flow for the intermediate circuit.

$$p_M = \sqrt{p_H * p_L} \tag{15}$$

$$t_{M\_Low} = \frac{t_{S_{Low}} + t_{R_{Low}}}{2} = t_{sat}(p_M, Ref) \tag{16}$$

When integrated appropriately, the system can achieve COP_{total} values up to 25% higher than those of a single-stage central HP ($COP_{single-stage}$) for the same temperatures at source- and sink-side. This requires that the central basic HP is dimensioned sufficiently large, as it must extract at least the same source-side thermal power as the single-stage configuration. Achieving even higher COP values necessitates a further increase in source-side heat extraction. The required compressor swept volume (V_{swept}) is dictated by the thermodynamic conditions at the suction state, particularly by the refrigerant density at the compressor inlet (Eq. 17). Due to the higher liquid fraction at the inlet of the evaporator of the basic HP, the necessary V_{swept} for a given source-side heat extraction can be reduced. This reduction arises from the increased enthalpy difference achievable in the evaporator (Δh_{eva}, see Fig. 13) compared to a single-stage cycle (Eq. 18).

[4] For improved clarity, the cycles were redrawn and graphically streamlined rather than shown solely as raw simulation outputs in the T/h or log p/h diagrams. The direct simulation results are summarized in the tables and illustrated with representative examples in Figures 13 and 14.

$$V_{Swept} = \frac{\dot{m}_{ref,basic}}{rpm * \rho_1 * \eta_{vol}} \quad (17)$$

$$\dot{Q}_0 = \dot{m}_{ref} * (\Delta h_{eva}) \quad (18)$$

A detailed simulation study using EES [11], for the refrigerant propane (R290) for both basic and booster was used., For the simulation, an isentropic efficiency of 80%, for each compressor was used. The swept volume of the basic compressor was set to 42 ccm and volumetric compressor efficiency of 80%, the one of the booster si set to 20 ccm and the volumetric compressor efficiency of 70%,, the pinch-point temperature difference of the basic is 5 K and for booster is 3 K, as well as superheating temperature of 5 K are an oil ratio of 10% and a mechanical-electrical efficiency of 92% assumed; for both rotational speed is set point of the simulation but could be adapted to required heat capacity (with maximum of 7200 rpm), as well as required mass flow of air and heating water circuit. The boundaries set in the simulation are a fixed return and supply temperatures and air source inlet temperature as well. For the booster the rpm is adapted that the heat source temperatures in and outlet fit to fit the heat sink temperatures.

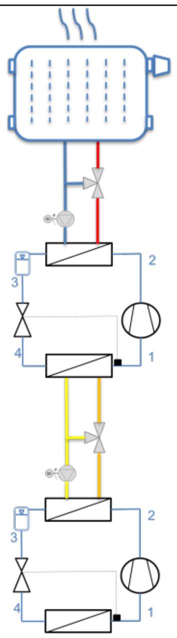

Figure 7: Schematic of a Booster/Basic- heat pump system for radiator heating with intermediate circuit

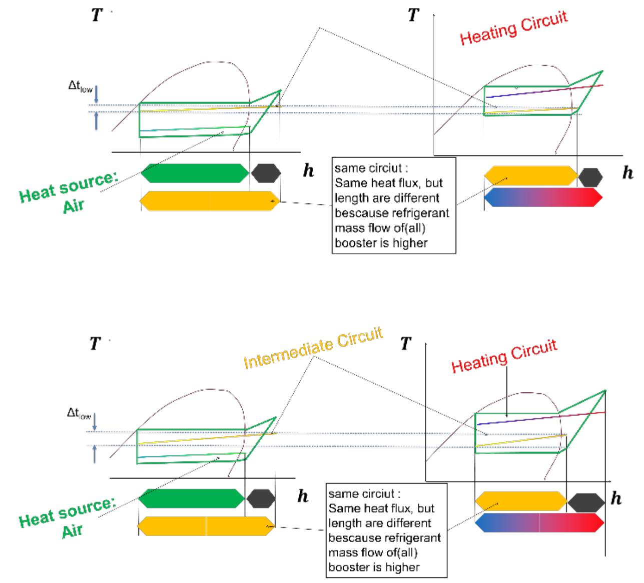

Figure 8: Basic-booster vapor-compression heat pump cycles with the same refrigerant represented in the temperature–enthalpy (T–h) diagram, including the temperature levels of the heat sink (blue/red), the low-temperature heating circuit (intermediate circuit/orange), and the heat source (green).

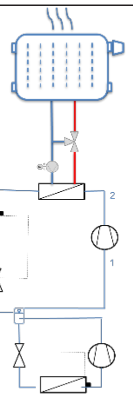

Figure 9: Schematic of a two-stage-heat pump system for radiator heating with intermediate circuit [10]

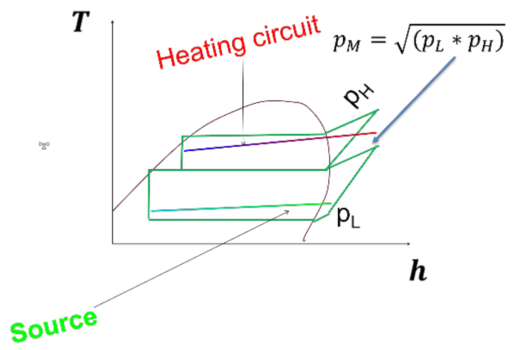

Figure 10: Two-stage vapor-compression heat pump cycle represented in the temperature–enthalpy (T–h) diagram, including the temperature levels of the heat sink for radiator heating. [10]

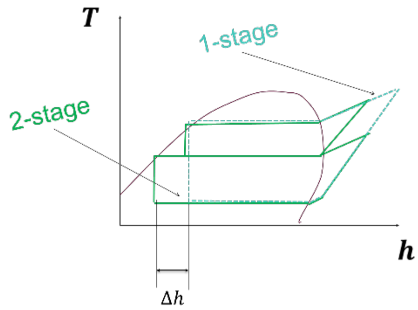

[5]

Figure 11: Comparison of the two-stage with a single-stage vapor-compression heat pump cycle represented in the temperature–enthalpy (T–h) diagram, showing the extra enthalpy gain in the 2-stage evaporator due to the higher liquid fraction after the expansion valve

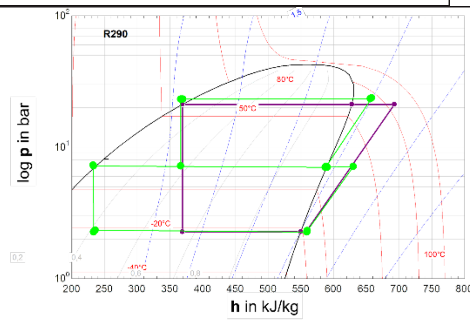

Figure 12: Simulation result (EES) of the comparison of the two-stage with a single-stage vapor-compression heat pump cycle represented in the temperature–enthalpy (logp–h) diagram, showing the extra enthalpy gain in the 2-stage evaporator due to the higher liquid fraction after the expansion valve

3.3. Comparison of basic-booster HPs with a two-stage heat pump

In particular, a thermal energy storage tank in the low-temperature circuit could be used (see Figure 15) to operate the basic HP at higher outside air temperatures during the day and thus achieve higher COPs. At night, the apartments are heated exclusively by the booster HPs, without the basic HP being operated, using the energy from the storage tank as heat source. So, the low-temperature storage tank serves as the source at night and therefore allows a day night shift. For example, the average temperature difference in Vienna in winter is 5 K higher at daytime than at nighttime [5].

A further big advantage of using the thermal energy storage (TES) in the intermediate level is that the temperature level is quite low (about 20 °C). The TES is often located in the basement or in the attic, so that the temperature difference between the TES and the surrounding air (ca. 15 °C) is very small. But, considering the required low temperature spread (Δt) in the intermediate heat transfer circuit, the TES requires a big volume according to Eq. 19 [10]. However, the simulation analysis showed that if this temperature difference is exploited (see Table 2, and Fig. 14 (heat capacity is set to 10 kW for all different solution, so COP, the electrical power consumption and the required source temperature is changing), the overall COP_{total} can be increased by another 10%.

$$V_{TES} = \frac{Q}{\rho_1 * c_p * \Delta t} \qquad (19)$$

[5] For improved clarity, the cycles were redrawn and graphically streamlined rather than shown solely as raw simulation outputs in the T/h or log p/h diagrams. The direct simulation results are summarized in the tables and illustrated with representative examples in

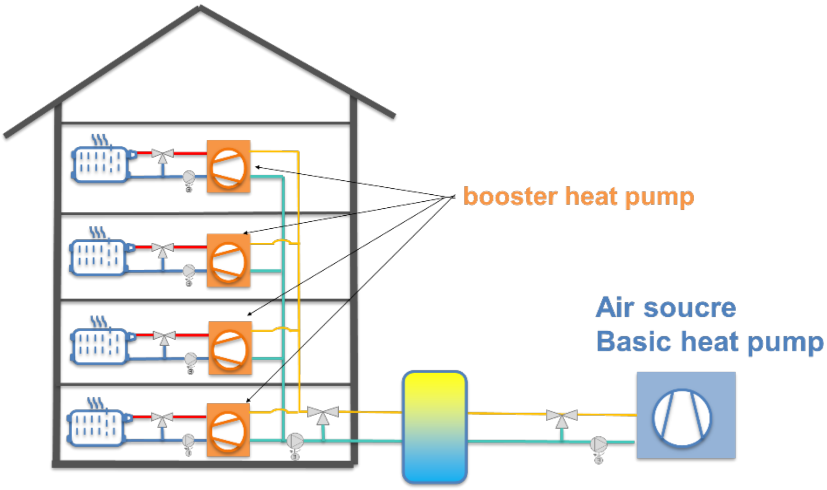

Figure 13: Schematic of one centralized heat pump as basic heat pump and booster heat pumps plus intermediate thermal energy storage in each flat as HP concept for multi-storey residential buildings with radiators [10]

Table 2. Comparison of the COPs of booster and basic heat pumps, individually and in combination, at different outdoor temperatures (day/night)

	Basic-HP @ night	Basic-HP @ day	Booster-HP
Average sink temperature in °C	20	20	45
Average source temperature in °C	-10	-5	20
COP	3,9	4,7	5,1
COP_{total}	2,5	2,7	

Because the basic heat pump does not run at night, the nighttime noise pollution caused by the air source blower of the outdoor air heat pump can also be avoided.

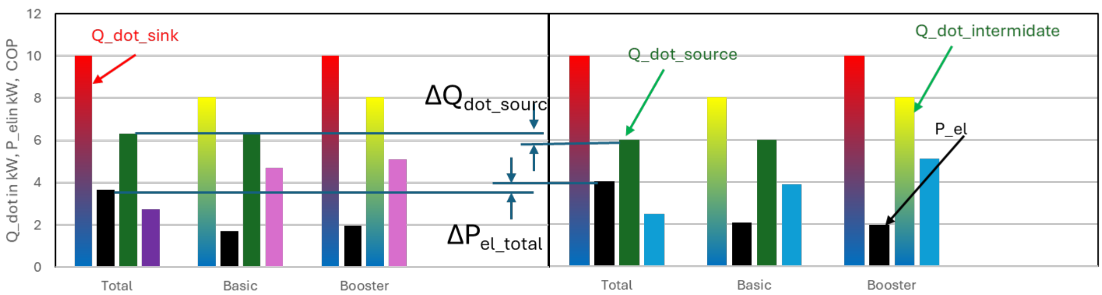

Figure 14: Electrical power input (in black), heat sink (blue/red), the low-temperature heating circuit (intermediate circuit/orange), and the heat source (green). and coefficient of performance (COP) of the cascade heat-pump system at two ambient temperature conditions. The left panel shows operation at −5 °C, the right panel shows the day at −10 °C. For each condition, results are presented for the total cascade system and disaggregated into contributions of the basic heat pump and the booster heat pump. Conditions are listed in Table 2

4. Conclusion

This work demonstrates that basic-booster heat pump configurations, in combination with targeted thermal refurbishment measures, allow efficient low-temperature operation in existing radiator-based heating systems. The comparative analysis of the investigated configurations shows that the proposed intermediate heating circuit significantly improves system performance while maintaining moderate compressor power and auxiliary heat demand. The results indicate that such system concepts offer a technically viable and scalable solution for the decarbonization of existing urban building stocks where full heating system replacement is impractical. The basic-booster heat pump systems operate in a staged network and are a strong option achieving high temperature lifts, as required in the case. If the same refrigerant is used for both the basic-booster heat pump system, the maximum COP is limited under the two-stage cycle. With proper integration, COP can be increased by 25% compared to single-stage central heat pumps at same conditions. This is because evaporation in the basic heat pump starts with a higher liquid fraction, as the inlet pressure is lower at approximately 20 °C compared to the single-stage system, which operates at around 45 °C. However, the central basic heat pump must be large enough to absorb the required heat source from the air. Higher COPs mean that for the same heating capacity more energy comes from the heat source than from electricity. The ideal temperature level of the low-temperature circuit depends on the medium pressure level of the two-stage cycle for the same temperature levels (and lift and refrigerant), with the spread kept as small as possible.

Furthermore, an intermediate storage tank can be used to shift the higher outside air temperatures from day to night, allowing the booster heat pumps to be operated without running the basic heat pumps. The average temperature difference in Vienna COP can increase by around 10% compared to a system without a buffer tank can be achieved. This is also helpful in avoiding nighttime noise pollution from the air source fan. However, if the hydraulic system is correctly designed and properly controlled, basic-booster heat pumps represent an energy-efficient substitution technology for natural gas-fired single-storey boilers in renovation projects.

It is important that in the case of existing pump remains, the thermal renovation and the resulting reductions in the heating load and heating demand also change the return temperature and the spread tends to become smaller. This will also have an influence on the individual room regulation. Above all, attention must be paid to the correct control strategy of the complex system when the supply temperature adjusts according to the heating curve. In partial load, the optimal temperature level for the intermedia circuit and TES also changes. Further studies will have to show whether it makes sense to adapt this into the control.

Nomenclature

	Description	Unit
A	heat transfer area of the heat exchanger	m^2
ACH	air change rate	h^{-1}
COP	coefficient of performance	$-$
c_p	(isobaric) specific heat capacity	$kJkg^{-1}K^{-1}$
DH	district heating	kW
$\dot{Ex}$	exergy flux	kW
$\dot{Ex}_{irr}$	exergy losses	kW
h	enthalpy	$kJkg^{-1}K^{-1}$
HTC	heat transfer coefficient	$Wm^{-2}K^{-1}$
$\dot{m}$	mass flow rate	kgs^{-1}
$\dot{m}_{ref}$	refrigerant mass flow rate	kgs^{-1}
m	mass	kg
n	heat-emission exponent	$-$
p	pressure	Pa
p_H	high pressure side	Pa
p_M	intermediate pressure side	Pa
p_L	low pressure side	Pa
P_{el}	electrical power	kW
$\dot{Q}$	heat capacity, heat flux	kWm^{-2}
$\dot{Q}_H$	heat flux emitted from the HP to the heating circuit (sink)	kWm^{-2}
$\dot{Q}_L$	heat flux for the infiltration heat losses of a building	kW/m^{-2}
$\dot{Q}_0$	heat flux absorbed to the HP (source)	kWm^{-2}
$\dot{Q}_T$	heat flux for the transmission heat losses of a building	kWm^{-2}
rpm	rotational speed of the compressor	s^{-1}

s	entropy	$kJkg^{-1}$
SPF	seasonal performance factor	$-$
T, t	temperature	$K, °C$
T_a	ambient temperature	$°C$
TES	Thermal Energy Storage	
t_i	room temperature	$°C$
t_R	return temperature	$°C$
t_S	supply temperature	$°C$
t_{sat}	saturation temperature	$°C$
U	heat transmission coefficient	$Wm^{-2}K^{-1}$
$\dot{V}$	volume flow rate	m^3s^{-1}
V	volume	m^3
ΔT_{PP}	pinch-point temperature difference	$°C$
Δt	temperature spread	K
ρ	density	kgm^{-3}

References

[1] Mitterrutzner M, Prada A, Lazzarin R, Corrado V. Review of heating and cooling technologies for buildings: A techno-economic analysis of eleven European countries. Energy Build 2023;292:113207.

[2] Naumann S, Kaltschmitt M, Kluge T. Environmental and economic assessment of residential heating systems for a German two-storey dwelling. *Sustain Prod Consum* 2024;40:112–28.

[3] Mancini, Francesco & Nastasi, Benedetto. (2019). Energy Retrofitting Effects on the Energy Flexibility of Dwellings. Energies. 12. 2788. 10.3390/en12142788.

[4] Zotter G, Ochs F. *"PhaseOut – How to Successfully Achieve the Natural Gas Exit"* TGA, Wien, 15.09.2022. Available at: https://tga.at/errichten/phaseout-so-gelingt-der-gasausstieg/ (in German: PhaseOut – so gelingt der Gasausstieg)

[5] Rudonja, N., Gojak, M., Zlatanović, I., & Todorović, R. (2020). Thermodynamic Analysis of a Cascade Heat Pump Incorporated in High-Temperature Heating System. Strojniški vestnik - Journal of Mechanical Engineering, 66(11), 677-683. doi:http://dx.doi.org/10.5545/sv-jme.2020.6836

[6] Yixiu Dong, Ruzhu Wang. When and how to use cascade high temperature heat pump—Its multi-criteria evaluation, Energy Conversion and Management, Volume 309, 2024, 118435, ISSN 0196-8904, https://doi.org/10.1016/j.enconman.2024.118435.

[7] Naumann, Gabriel & Schropp, Elke & Gaderer, M.. (2024). Environmental, economic, and eco-efficiency assessment of residential heating systems for low-rise buildings. Journal of Building Engineering. 98. 111074. 10.1016/j.jobe.2024.111074.

[8] Lorenz, H. Assessment of Refrigeration Machines, Z VDI, 38 (1894), pp. 124-130, 62–8, 98–103 (in German: Beiträge zur Beurteilung von Kühlmaschinen)

[9] Gerald Zotter, Bernhard Adler; Andreas Längauer. A novel heat pumping cycle in a rotation heat pump for latent process heat supply using sensible heat sources Proceedings of IIR Gustav Lorentzen Conference on Natural Refrigerants, College Park, Maryland, USA, 2024, DOI:10.18462/iir.gl2024.1113

[10] Zotter, G.. Efficient Booster & Basic Heat Pump Concepts for Renovation, in Proceedings of enova-conference, 2023, Austria (in German: Effiziente Booster/Basic-Wärmepumpen-Konzepte für die Sanierung)

[11] EES (2022): Engineering Equal Solver, Version: 11.469

[12] Kleefkens, O., Berkel, J. V., Geelen, C.P.J.M., Bos M. (2017): Booster Heat Pump, development of test procedure and calculation methodology in order to estimate the energy performance in various domestic applications, in Engineering, Environmental Science at HPC 2017, Published 2017, Corpus ID: 201727202

[13] Zhu T., Ommen T., Meesenburg W., Thorsen J.E., Elmegaard B. (2021): Steady state behavior of a booster heat pump for hot water supply in ultra-low temperature district heating network, Journal of Energy, Volume 237, 2021, 121528, ISSN 0360-5442, https://doi.org/10.1016/j.energy.2021.121528.

[14] Masip, X., Prades-Gil, Emilio Navarro-Peris, C. Corberán , J.M. (2021): Evaluation of the potential energy savings of a centralized booster heat pump in front of conventional alternatives, Smart Energy, Volume 4, 2021, 100056, ISSN 2666-9552,

[15] Bauer C. (2022): Daily temperature variation – The difference between day and night, Vienna city (in German: Der Tagesgang der Temperatur – Der Unterschied zwischen Tag und Nacht, Stadt-Wien, https://www.stadt-wien.at/freizeit/wetter/tagesgang-temperatur.html)